Multi-body Space Structures

Adams Assignment Report

A.Y. 2022/2023

Payload Release

Alessandro Latini, Martina Marrocco, Valentina Piccione

June, 2023

Introduction

This document is the report for the Hexagon Adams assignement of Multi-body Space Structures course, held by Professor Michele Pasquali, from the Aerospace Engineering MD at the University of Rome Sapienza.

1 Problem description

The model is composed of an upper stage and two spacecrafts with different masses and inertias. The upper stage starts to spin as soon as the two thrusters on it are ignited, and a release mechanism is used to separate the spacecrafts from the upper stage. The deployment must ensure the following requirements:

- The maximum time duration of the simulation must be 10s
- The maximum spin rate of the payloads after the deployment must be lower than 5 deg/s at least
- The nutations must be minimized
- The minimum distance between the two payloads must be at least 1m at the end of the simulation in order to avoid collisions and interference between the two.

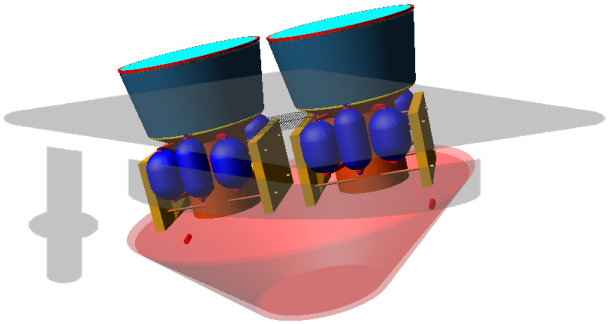

Figure 1: Model geometry

The objective of the assignment is to model the payload release mechanism through the use of Hexagon Adams Software. To this aim, it is required to define the forces acting on the system, such as: the thruster forces acting on the upper stage, the tiedowns acting between the two payloads and the upper stage, and the push-off springs forces needed for the separation of the payloads from the upper stage. These forces must be such as to fulfill the requirements.

2 Design Variables (DVs)

In the model different design variables have been introduced in order to simplify and parametrize the different functions used to define the forces. The first design variable is the `DV_Student = 0.15` and it has been considered as fixed because its only purpose is to change the mass and the inertia of the two payloads. It is also possible to set even the mass ratio parameter between the payloads for which the design variable has been defined as `DV_payls_mass_ratio = 1.5`.
Other design variables have been introduced, such as:

- `DV_wz`: the desired upper stage angular velocity along z-axis.
- `DV_thrust`: the module of the thruster forces.
- `DV_tiedown_K` and `DV_tiedown_D`: respectively the stiffness and the damping coefficient of the tiedown forces.
- `DV_tiedown_Kt` and `DV_tiedown_Dt`: the rotational stiffness and the rotational damping coefficient of the tiedown torques.
- `DV_spr_K` and `DV_spr_preload`: the stiffness and the preload of the spring force that push the payloads away from the upper stage.
- `DV_release_time_start_dx` and `DV_release_time_start_sx`: respectively the time instants at which the right and the left payload are released from the upper stage.
- `DV_release_time_span`: the (infinitesimal) time interval needed to disactivate the tiedown forces and to allow the payload separation from the upper stage.

3 Thruster forces

The thrusts, given by the two thrusters on the upper stage, have been modeled as the sum of a constant function and an `IF` function as follows:

```
1 DV_thrust + IF(.Payload_Release.upperstage_wz+.Payload_Release.DV_wz:
2 -DV_thrust,0,0)
```

The constant function "`DV_thrust`" represents the intensity of the force which has been applied to the origin of the marker located in the thruster, while the `IF` function is needed so that, when the desired angular velocity along the z-axis, represented by `DV_wz`, is reached by the upper stage, the thrusts go to zero so to maintain the upper stage angular velocity around the z-axis constant.

The choice to have two thruster forces with the same modulus is arbitrary, even though it has been noticed and taken into account in the further development of the project that the right thruster's x-axis is not parallel to that of the left one. This fact implies two main consequences:

- The center of mass of the upper stage is not on the geometric symmetry axis, that, also, is not perfectly aligned to one of the inertia principal axis.
- The thrusts are not mutually balanced in order to generate a simple torque around the symmetry axis, but there are also small unbalanced components of these forces that are one of the main causes of the transversal rotation.

4 Tiedown forces

The tiedown forces have been modeled using a general force vector ($GFORCE$), so to have components for both force and torque on all axis. They are differentiated between right and left payload and are modeled as functions of displacements, velocities and time. The action part is always the payload and the reaction part is the upper stage. As their application points, the origins of the frames located in corrispondence of the payloads bases (see markers present in the payloads geometry in the model, named `Tiedown_sx` and `Tiedown_dx`) have been chosen.

Their behaviour has been modeled as bushing-like functions in all the 3D-space directions, both translational and rotational. The stiffness and damping coefficients must be sufficiently large in

order to ensure that the payloads keep themselves attached to the upper stage and with a fixed orientation with respect to it, counteracting the thrusters and centrifugal forces exerted on them. This kind of force for the tiedowns has been chosen to simulate as realistically as possible the action of a rigid constraint that fix two bodies between themselves.

In this way, the component of the tiedown force for the right payload along the x-axis of the frame `upper_stage.tiedown_dx`, for example, is given by:

```
-DV_tiedown_K*DX(Payload_dx,upper_stage.tiedown_dx,upper_stage.tiedown_dx)
-DV_D*VX(Payload_dx,upper_stage.tiedown_dx,upper_stage.tiedown_dx,upper_stage.
    tiedown_dx)
```

Furthermore, the tiedowns actions are designed in such a way that their forces and torques must be deactivated (using a `STEP` function) after a certain time (`DV_release_time_start_payload`) and almost istantly (`DV_release_time_span`, that has to be very small), so that the payloads are free to be pushed-off. The `STEP` function is modeled in the following way:

```
STEP(time,DV_release_time_start_sx,1,DV_release_time_start_sx+DV_release_time_span,0)
```

The total force has been modeled as the product of these two fuctions. The same has been done for the components of the forces and torques along all the axes and for both right and left payload.

5 Push-off springs forces

To deploy the payloads the push-off spring force has been implemented using a force vector ($VFORCE$). In this way this force is defined only by its components on three axes. In particular the x and y components are put equal to 0, while the z component is different from 0 in order to push the payload up along the z-axis making them separate from the upper stage. This type of forces has been modeled using an `IF` function.

The z component function of the right payload is implemented as follows:

```
IF(DZ(Payload_dx.spr_dx,upper_stage.spr_dx,upper_stage.spr_dx)-DV_spr_preload:
-DV_spr_K*DV_payls_mass_ratio*(DZ(Payload_sx.spr_dx,upper_stage.spr_dx,upper_stage.
    spr_dx)-DV_spr_preload)
```

The `IF` function for the right and left payload differs for the parameter `DV_spr_K`. In fact, this function is multiplied by the mass ratio parameter for what concerns the right payload, since it is the payload with higher mass, in order to scale the push-off force and deploy the two payloads together, making them reach almost the same distance from the upper stage.

6 Optimization

Once all the forces acting on the system have been defined, a simulation has been done to make sure the release mechanism would work as expected.

The Tab.1a shows the values of the Design Variables for the first simulation, which were chosen following some reasonable criterions in order to obtain a correct performance of the mechanism. In particular, for the DVs related to the stiffnesses and the damping coefficients of the tiedown forces, high values have been assigned to them from the beginning, in order to better simulate the behaviour of a constraint able to fix rigidly two bodies, while, for the DVs of the release springs, the established values are such as to satisfy the requirements.

Furthermore some measures, such as the payloads angular velocity around all the three directions, the payloads distance and the payloads separation distance from the upper stage at the end of the simulation, have been evaluated to ascertain that the requirements had been satisfied.

The measures in Tab.1b have been defined as follows:

1. **`payl_dx_WX_inerz`** and **`payl_sx_WX_inerz`**: respectively the right and left payload angular velocity around the x-axis (nutation around x-axis) measured with respect to the inertial reference frame.

2. **payl_dx_WY_inerz** and **payl_sx_WY_inerz**: respectively the right and left payload angular velocity around the y-axis (nutation around y-axis) measured with respect to the inertial reference frame.
3. **payl_dx_WZ_inerz** and **payl_sx_WZ_inerz**: respectively the right and left payload angular velocity around the z-axis measured with respect to the inertial reference frame.
4. **payl_dx_WN** and **payl_sx_WN**: measures defined by the following formula: $\sqrt{(w_x)^2 + (w_y)^2}$ to represent simultaneously the nutations' variations for the right and left payload.
5. **payload_distance**: the bigger distance between the two payloads at the end of the simulation measured between the two external points on the two payloads: one belonging to the left payload's *SOLID53* and the other one belonging to the right payload's *SOLID52*, as it can be seen in Fig. 2.

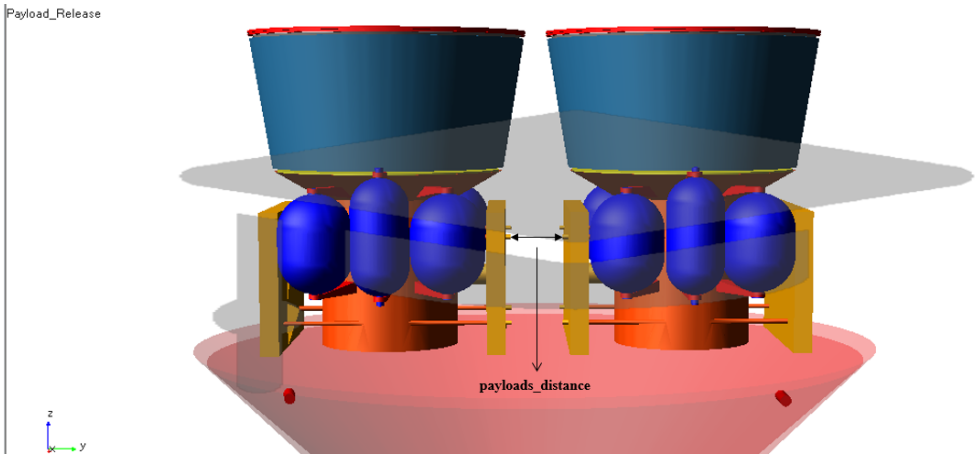

Figure 2: Representation of the `payload_distance` measure on the model

6. **payload_distance2**: the smaller distance between the two payloads at the end of the simulation measured between the two external points taken at the edge of the two payloads' *SOLID5*, as it can be seen in Fig. 3.

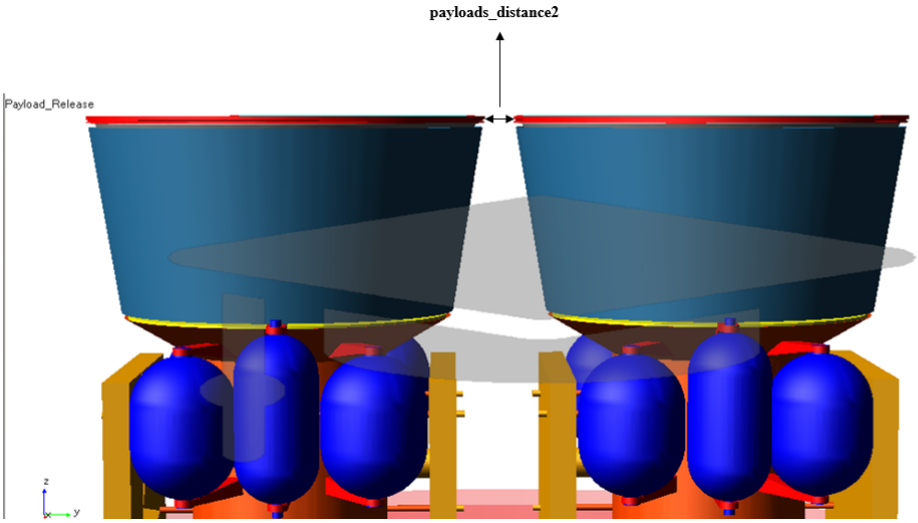

Figure 3: Representation of the `payload_distance2` measure on the model

7. **DZ_payldx_upperstage** and **DZ_paylsx_upperstage**: the distances from the upper stage of the right and left payload, respectively.

DV_thrust [N]	300
DV_wz [deg/s]	4.8
DV_tiedown_D [N s/mm]	1e6
DV_tiedown_K [N/mm]	1e7
DV_tiedown_Dt [N mm/deg]	1e6
DV_tiedown_Kt [N mm s/deg]	1e7
DV_spr_K [N/mm]	1.2
DV_spr_preload [mm]	50
DV_release_time_dx (& sx) [s]	2.5
DV_release_time_span [s]	0.01

(a) Design Variables

payl_dx_WX_inerz [deg/s]	-0.03592
payl_sx_WX_inerz [deg/s]	-0.03533
payl_dx_WY_inerz [deg/s]	-0.2153
payl_sx_WY_inerz [deg/s]	-0.2155
payl_dx_WZ_inerz [deg/s]	-4.992
payl_sx_WZ_inerz [deg/s]	-4.992
payl_dx_WN [deg/s]	0.2183
payl_sx_WN [deg/s]	0.2183
payload_distance [mm]	1226
payload_distance2 [mm]	862.2
DZ_payload_upperstage_dx [mm]	1529
DZ_payload_upperstage_sx [mm]	1488

(b) Measurements

Table 1: Tables of the chosen design variables, 1a, and the measurements obtained, 1b, carried out after the first simulation.

As it could be noticed from Tab.1b all the requirements have been met except that regarding the smaller measured distance between the payload (defined by `payload_distance2`), which is still under 1m distance.

Furthermore, it could be observed that the payloads nutations about the y-axis is bigger than that around the x-axis. In spite of this, our further goal is to minimize both nutations because, even though the nutation around x-axis is smaller than the other one, it is the one which could be more responsible for the possible risk of collision between the two payloads.

Due to this fact a parametric analysis and investigation shall be carried out in order to optimize the model. To this aim it was necessary to define some objectives (OBJs).

6.1 Objectives definitions

In total twelve objectives have been defined in order to meet the requirements and they could be divided in two categories: the first one includes the objectives regarding the minimization of the payloads nutations, always taking into account the need to increase the smaller distance between the payloads, and the other one includes those objectives which have been defined to check whether the remaining requirements are still satisfied after the optimization.

1. **`max_WN_dx`** and **`max_WN_sx`**: the **maximum absolute value during simulation** of the measure `WN` for both payloads.
2. **`end_DZ_payldx_upstage`** and **`end_DZ_paylsx_upstage`**: the **value at simulation end** of the distances between the basis of the payloads and the upper stage.
3. **`end_payload_distance`**: the **value at simulation end** of the measure **`payload_distance`**.
4. **`end_payload_distance2`**: the **value at simulation end** of the measure **`payload_distance2`**.
5. **`max_WX_dx`** and **`max_WX_sx`**: the **maximum absolute value during simulation** of the payloads nutation angular velocity around x-axis.

6. **max_WY_dx** and **max_WY_sx**: the **maximum absolute value during simulation** of the payloads nutation angular velocity around y-axis.

7. **max_WZ_dx** and **max_WZ_sx**: the **maximum absolute value during simulation** of the payloads angular velocity around z-axis.

6.2 Objectives results

FIRST STRATEGY AND OPTIMAL ONE

The first strategy, that has been followed to try to optimize the model, is based on the fact that its goal is to minimize the payload nutations' values always guaranteeing the requirements' fulfillment.

For these reason the first two aforementioned Objectives, those regarding the minimization of the payloads nutations, have been used to carry out different DoEs, whose aim is first, to identify which design variables, between all those already defined, have the bigger influence on the nutations and second, which values of those permits to reach the optimal value for the payloads nutations. All this has been done always taking into account that all the requirements had to be fulfilled at the same time. For this reason,the spin angular rate has been increased and updated in the `(DV_wz)` (from the value of 4.8 deg/s to the 4.95 deg/s, near to the maximal acceptable one) because this allows to make the distance between the payloads larger, since there is a proportional relationship between these two.

From these DoEs it is apparent that the Design Variables referring to the release time of the two payloads `(DV_release_time_start_dx)` and `(DV_release_time_start_sx)` are those that mainly influence the behaviour of the measurements since the payloads release strategy is based on them, for how it has been defined through the forces.

Due to this fact, more DoEs, which objectives were set to be `(max_WN_dx` and `max_WN_sx)` for the left and right payload, have been carried out in order to find out which were the optimal values of the payloads release times that could minimize the most the nutations' values.

First, these DoEs have been examined taking into account that the release time DVs would change in a time interval whose minimum was 1s and the maximum 10s.
Secondly, it was possible to notice that reducing the payloads release time and setting it as equal for both payloads allowed the reduction of the nutations' values and a better accomplishment of the payloads' distance requirement. For this reason, the time interval, in which we make these DVs change, was further reduced below 1s (from a minumum of 0.01s to a maximum of 1s) in order to identify the best DVs values which would allow to obtain the optimal (i.e. minimal) payloads' nutations.

Furthermore, the thrust module has been increased and updated in the `DV_thrust` (from the value of 300 N in the initial simulation to the value of 500 N) in order to be able to reach the desired spin angular rate in a shorter amount of time than that needed to the payloads' release.

As a result of these first DoEs, it was apparent that the optimal values to be chosen for the payloads release time's Design Variables were equal to 0.1s. Due to this fact, the payloads release time's DVs have been properly updated and then, other DoEs (whose Objectives remains always the same as before) have been carried out in order to check now the influence of the upper stage spin angular velocity and the thrust on the nutations' values. After the latest DoE, the value of the upper stage spin angular velocity of 4.96 deg/s and the thrust module value of 500 N have been updated in the `DV_wz` and in the `DV_thrust`, respectively. They have been set in this way in order to get a good compromise between all the requirements, especially between the minimization of nutations and the maximization of the payloads distance, without exceeding the limit of the maximal spin angular velocity of 5 deg/s for the two payloads.

Despite all these considerations, it is not possible to obtain exactly the required minimal value of the smaller payloads' distance, i.e. `payload_distance2`, in the simulation time of 10s. For this reason it is necessary to increase the simulation time by a slightly amount of time (about 0.05s) to get it.

In fact, it can be verified that increasing the simulation time of about 0.05s, it is possible to reach 1.002m for the smaller distance (referring to `payload_distance2`), fulfilling the payloads' distance requirement completely.

SECOND STRATEGY

Beside to the previous main strategy, another one has been followed in order to minimize the nutations' values.
Unlike the previous one, the requirement regarding the distance between the payloads has been considered as regarding only the greater distance between the two, i.e. `payload_distance`. All this has been done always starting from the same initial Design Variables' values of the first simulation and changing only those regarding the release time and upper stage spin angular velocity.

In this way other DoEs have been done and what has been noticed is that we could reach an optimal value of the measure `W_N` (0.1495 deg/s for the left payload and 0.1746 deg/s for the right one) for a release time of 0.2575s and an upper stage spin angular velocity smaller than 4.8 deg/s.

In fact, it could be verified that decreasing the upper stage spin angular velocity until a value of 3.65 deg/s make the requirement fulfillment, regarding only the bigger distance between the two payloads, possible because the aforementioned distance has the exact value of 1m.

STRATEGY CHOICE

In spite of this second strategy the previous one was chosen as the optimal one just because it took into account a most accurate definition of the distance between the payloads.

In fact, even though with the first strategy we were not able to satisfy the aforementioned requirement (even though for a very little margin), we were however closer to its fulfillment than with the second strategy.

A further motive of choosing the first strategy regards the fact that, to fulfill the requirement regarding the smaller distance between the two payloads, the simulation time should be increased by a smaller amount than that needed with the second one. As a matter of fact, the simulation time shall be increased by at least 4s for the second strategy, which is far bigger that those 0.05s needed with the first and optimal one.

7 Final results

In conclusion, the final values of the DVs that allows to fulfill the requirements of the assignment are reported in Tab.2a. The changed values of the DVs with respect to Tab.1a are:

- `DV_thrust`
- `DV_wz`
- `DV_spr_preload`
- `DV_release_time_dx` & `DV_release_time_sx`

The other DVs that have been evaluated are less relevant than the previous ones for what concerns the purpose of the optimization, since their influence on the variability of the defined objectives is more or less neglectable.

As it can be seen from the Tab.2b, once the optimization has been done, both payloads nutation values around the x-axis have been reduced.

The same cannot be said for the left payload nutation value around the y-axis. In fact it has increased in comparison with the value carried out from the first simulation. Nevertheless, the important thing to notice is that, in spite of this, we were able to increase the distances between the two payloads, getting closer to the fulfillment of the requirement regarding the distance between the two payloads.

DV_thrust [N]	500
DV_wz [deg/s]	4.96
DV_tiedown_D [N s/mm]	1e6
DV_tiedown_K [N /mm]	1e7
DV_tiedown_Dt [N mm s/deg]	1e6
DV_tiedown_Kt [N mm s/deg]	1e7
DV_spr_K [N/mm]	1.2
DV_spr_preload [mm]	37.5
DV_release_time_dx (& sx) [s]	0.1
DV_release_time_span [s]	0.01

(a) Optimized Design Variables

payl_dx_WX_inerz [deg/s]	- 0.01855
payl_sx_WX_inerz [deg/s]	- 0.02226
payl_dx_WY_inerz [deg/s]	-0.1546
payl_sx_WY_inerz [deg/s]	-0.2938
payl_dx_WZ_inerz [deg/s]	-4.993
payl_sx_WZ_inerz [deg/s]	-4.993
payl_dx_WN [deg/s]	0.1557
payl_sx_WN [deg/s]	0.2947
payload_distance [mm]	1344
payload_distance2 [mm]	995.3
DZ_payload_upperstage_dx [mm]	1706
DZ_payload_upperstage_sx [mm]	1665

(b) Optimized measures

Table 2: Tables of optimized values for the Design Variables, 2a, and for the measures,2b

7.1 Final Measures

The measures regarding position, velocity, angle and angular velocity of the payloads center of mass (CoM) have been plotted in Adams through the utilization of the Post processor and then reported in the following subsections.

Due to the fact that those measures shall be carried out both in the global and local reference frame, they have been defined in the model with respect to an inertial and a local reference frame, respectively, with the last one centered in the upper stage CoM.

For what concerns the measures which shall be done with respect to the local reference frame centered in the upper stage CoM, the reference frame has to be specified in the measures definitions. Due to this fact, a *new* reference frame, always centered in the upper stage CoM, has been created in order to change the axis orientation of the already existing reference frame (called `upstage_cm_new` and present in the model under *Bodies* section in `upper_stage`). This was done just to be able to read the exact measures' components along the axes and so that these axes are parallel to those belonging to the payloads' reference frame centered in their CoMs.

7.2 Position and velocity of the payloads center of mass (CoM) globally and locally, with respect to upper stage CoM

As it can be seen from Fig.4 and Fig.6, the plots of the position of the payloads CoM along the x-axis and z-axis with respect to the inertial reference frame show monotonous trends in comparison with those of the same measure done with respect to the local frame. On the contrary, as it can be seen in Fig.5, the plot representing the position of the payloads CoM along the y-axis is constant in the inertial frame while the left payload shows a bigger deviation from its inertial trend than that of the right payload.
Looking at the inertial trends it can be seen that the two payloads are detaching themselves from the upper stage, mostly going up along z-axis in the same direction, due to the release springs' action, and secondly separating themselves along the x-axis in opposite directions, as it should be expected when an initial short rotation is applied, mainly along the z-axis, to the payloads, which are initially located along the y-axis. The main difference between the trends of the positions

with respect to the local frame and the ones with respect to the inertial one is represented by a deviation due to the rotation of the upper stage local frame around the z-axis.

For what concerns the velocity components of the payloads' CoM plotted in the inertial reference frame it can be seen that their trends are compliant with the previous plots representing the position's components of the payloads' CoM. In fact, the velocity components in the inertial reference frame along x-axis are constant and opposite in directions and those along the y-axis are constant and null, while the components along the z-axis are constant and with the same direction, pointing out the fact that the payloads are leaving the upper stage with a constant velocity after the first initial slope.

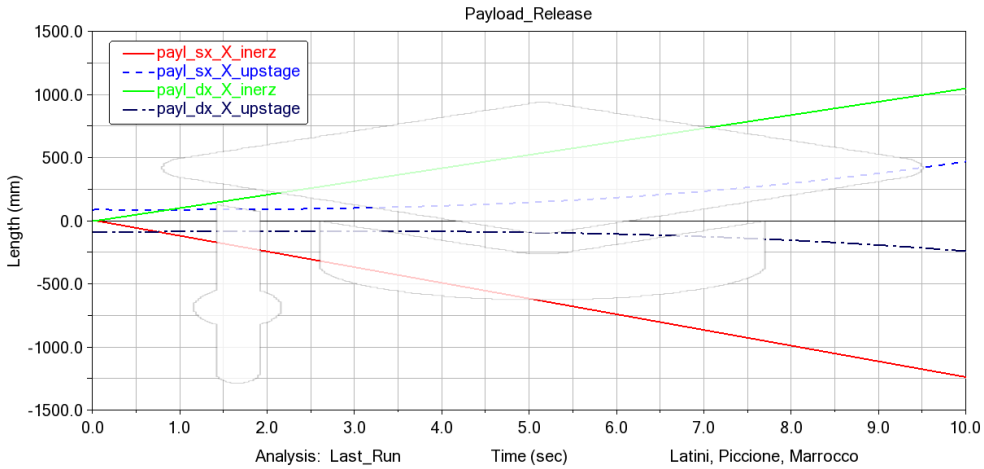

Figure 4: Position along the x-axis of the payloads CoM globally and locally, wrt the upper stage CoM

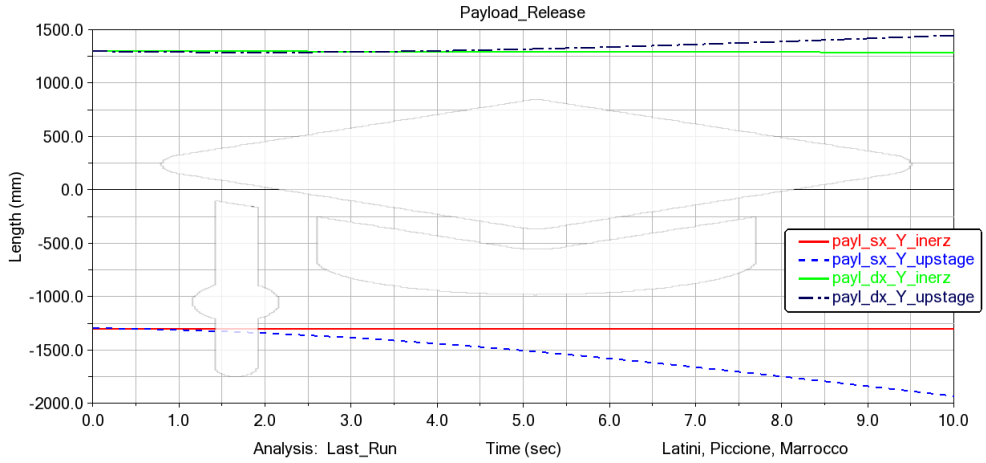

Figure 5: Position along the y-axis of the payloads CoM globally and locally, wrt the upper stage CoM

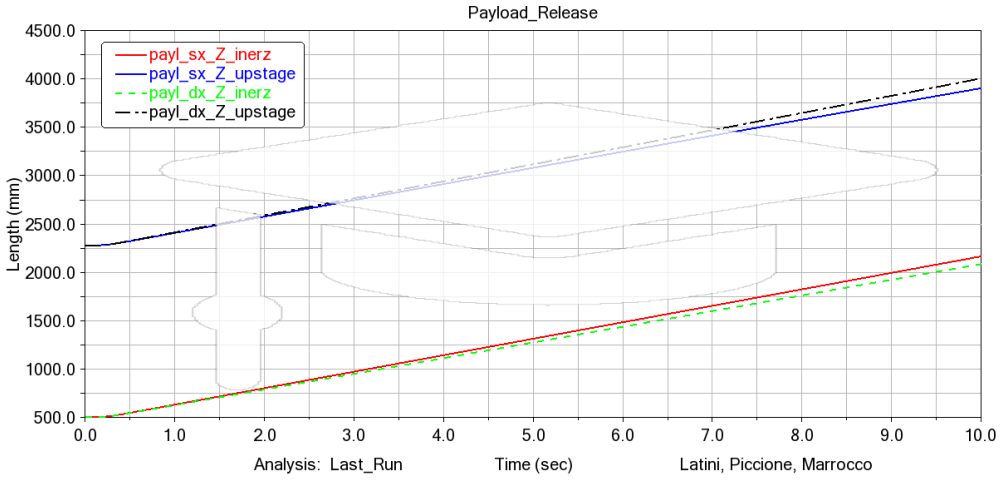

Figure 6: Position along the z-axis of the payloads CoM globally and locally, wrt the upper stage CoM

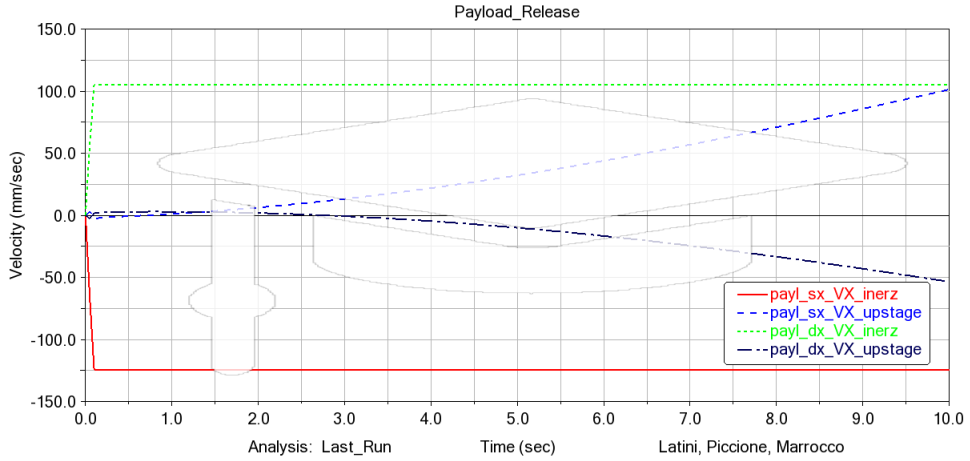

Figure 7: Velocity along the x-axis of the payloads CoM globally and locally, wrt the upper stage CoM

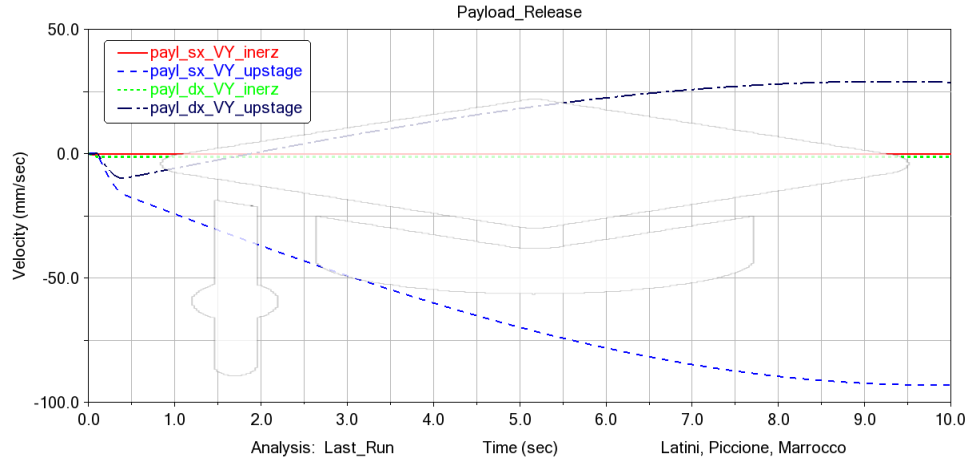

Figure 8: Velocity along the y-axis of the payloads CoM globally and locally, wrt the upper stage CoM

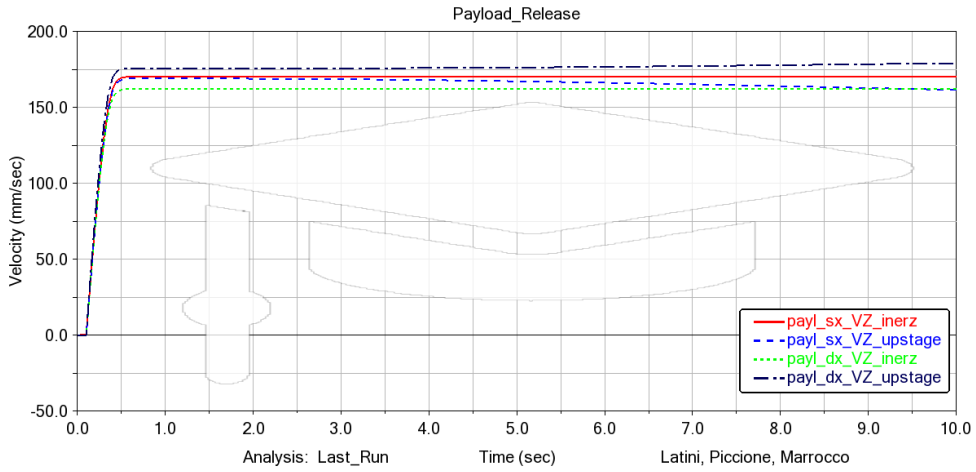

Figure 9: Velocity along the z-axis of the payloads CoM globally and locally, wrt the upper stage CoM

7.3 Angle and angular velocity of the payloads CoM globally and locally, with respect to upper stage CoM

As it can be noticed by the inertial trends of the angles represented in Fig.10, Fig.11 and Fig.12, the payloads rotate mostly around the z-axis and to a lesser extent around x and y-axis.

From a general point of view, the variations of the angles around the x-axis and y-axis, Fig.10 and Fig.11, are more or less of the same order of magnitude (under the threshold of 5deg), and are both smaller than the variation around the z-axis, exactly as it shall be expected.

Likewise, the payloads' inertial angular velocities occur in the same magnitude ratio of the angles, and so the variation around the z-axis is bigger than those around the x and y-axis, as it is shown in Fig.13, Fig.14 and Fig.15.

Furthermore, it also can be verified that the payloads spin angular velocity and the nutations' velocities around the x and y-axis keep almost constant during the simulation, after a very small initial slope, as it has already been reported numerically in Tab.2b in the paragraph 7.

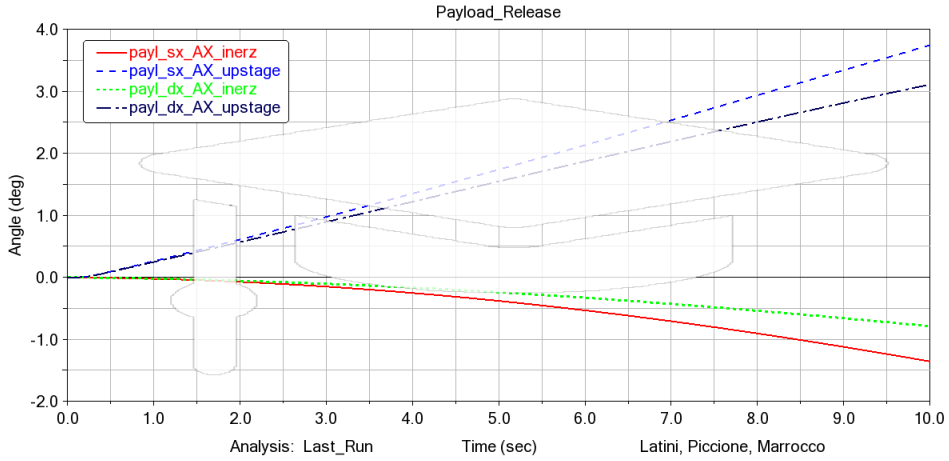

Figure 10: Angle around the x-axis of the payloads CoM globally and locally, wrt the upper stage CoM

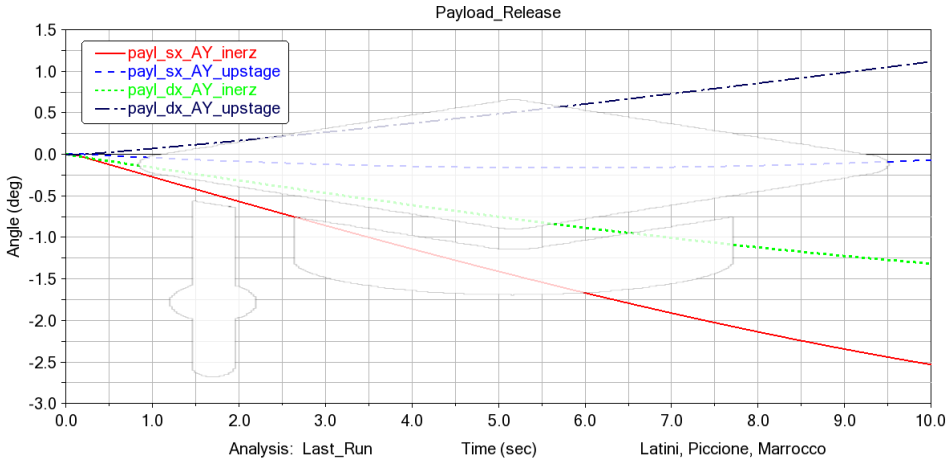

Figure 11: Angle around the y-axis of the payloads CoM globally and locally, wrt the upper stage CoM

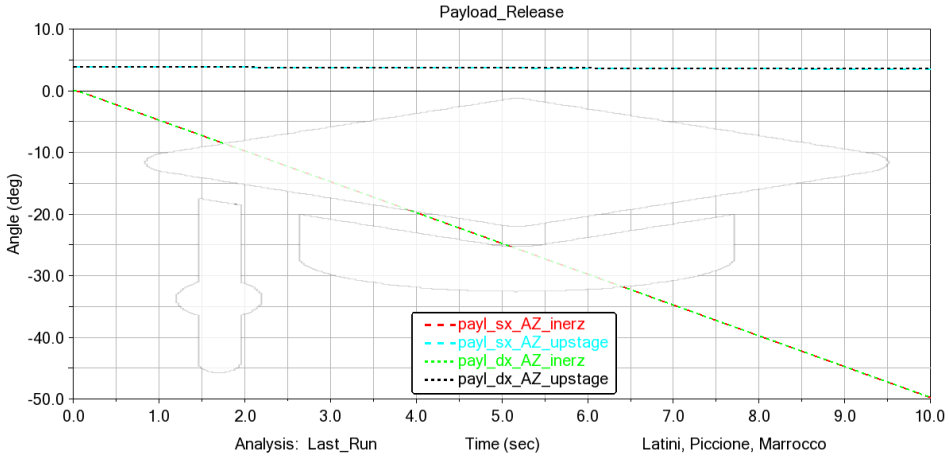

Figure 12: Angle around the z-axis of the payloads CoM globally and locally, wrt the upper stage CoM

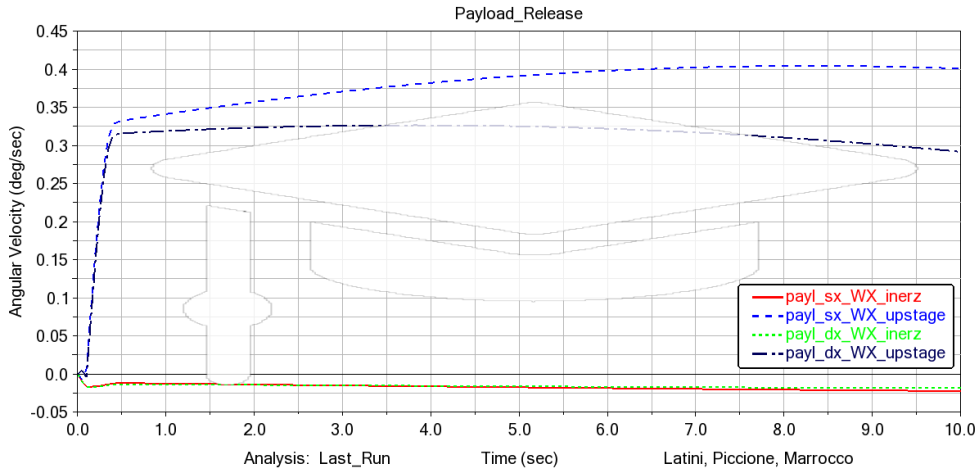

Figure 13: Angular velocity around the x-axis of the payloads CoM globally and locally, wrt the upper stage CoM

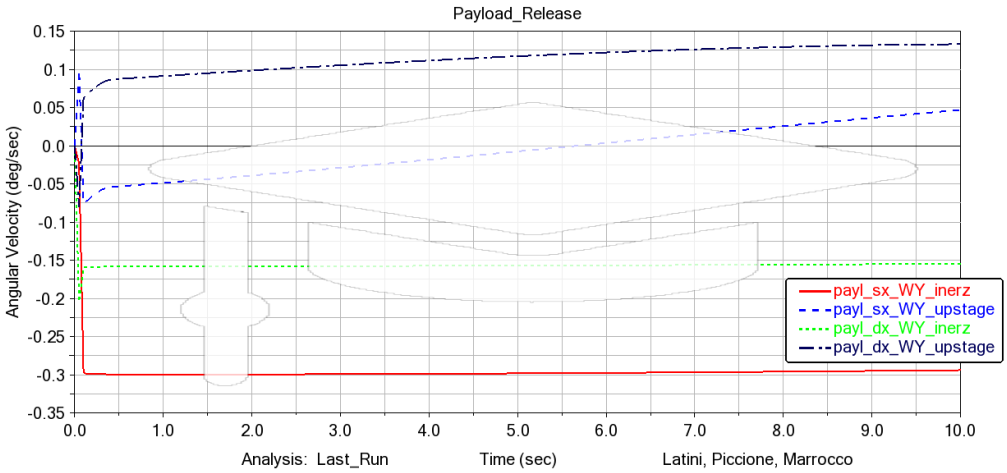

Figure 14: Angular velocity around the y-axis of the payloads CoM globally and locally, wrt the upper stage CoM

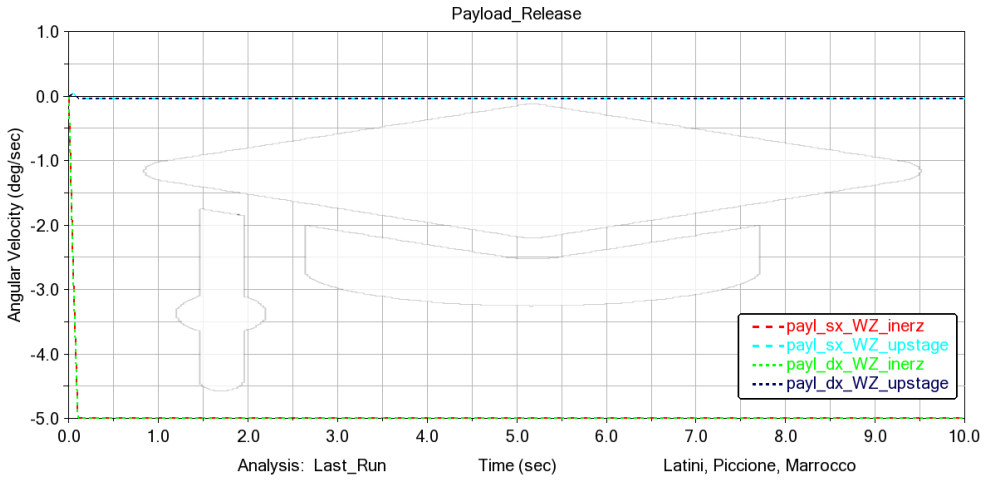

Figure 15: Angular velocity around the z-axis of the payloads CoM globally and locally, wrt the upper stage CoM

7.4 Forces components trends

From the behaviour of the components of the thruster forces in the Fig.16, Fig.17 and Fig.18, it is possible to verify that, first, their action lasts for a very short time because of the high value assigned to the module of thrust and, secondly, that the not perfectly alignment of the thrusters generates an unbalanced component along y-axis for the left one, although it is smaller than that of the main component along the z-axis, as it was predicted in the description of the thruster forces in the section 3.

The tiedown forces are the only forces that have been defined in the model so to have not null components of the torque, in order to counteract the relative rotational motion between payloads and upper stage during the phase in which they must be rigidly connected. The action time of these forces is very short due to the small release time and for this reason their oscillatory behaviour is not highlighted.

Regarding the forces of the tiedowns, which are shown in Fig.19, Fig.20 and Fig.21, the component along y-axis is negligible with respect to the others. In order to explain the reason for which this happens, it must be considered that the tiedowns' points of application are initially located along the y-axis and that their goal is to maintain the relative displacements between the upper stage and the payloads close to zero. Since the main variation of the relative displacements occurs

initially along the x-axis and the z-axis, the main action of the tiedown forces must be essentially along these two axes.

As it is shown in Fig.22, Fig.23 and Fig.24, the peak value in the graph of the tiedown's torque around z-axis is bigger than those around the x and y-axis, since the main component of the relative rotation that has to be nullified is exactly that along the z-axis.

As it is showed in Fig.25, Fig.26 and Fig.27, the release spring force's components along the x and y-axis are much smaller than that along the z-axis. In fact, their peak values are three order of magnitude smaller than that belonging to the component along z. This is justified by the fact that this type of force has been defined in such a way that its only purpose is to push the payloads far away from the upper stage, and this shall be done along the z-axis.

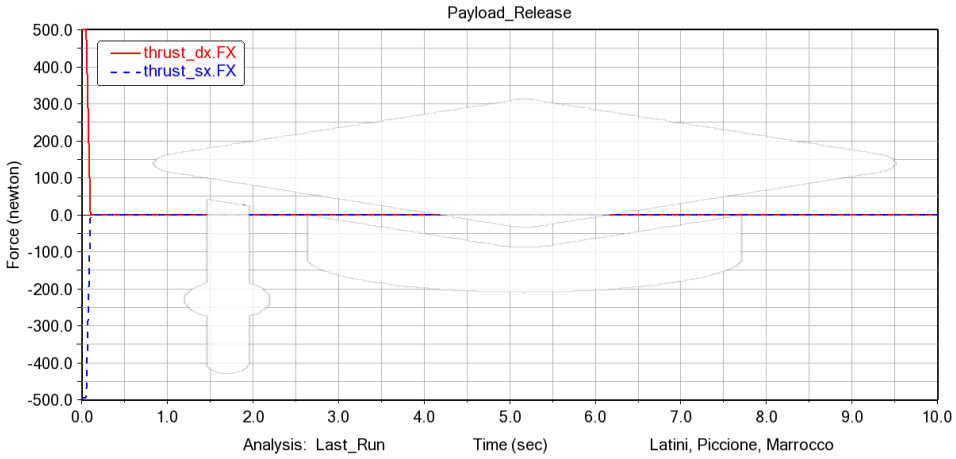

Figure 16: Thrusts components along the x-axis

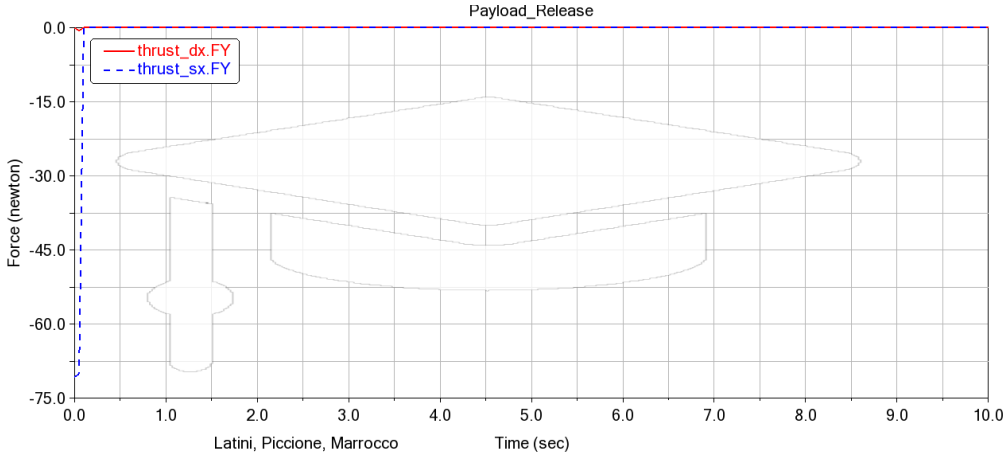

Figure 17: Thrusts components along the y-axis

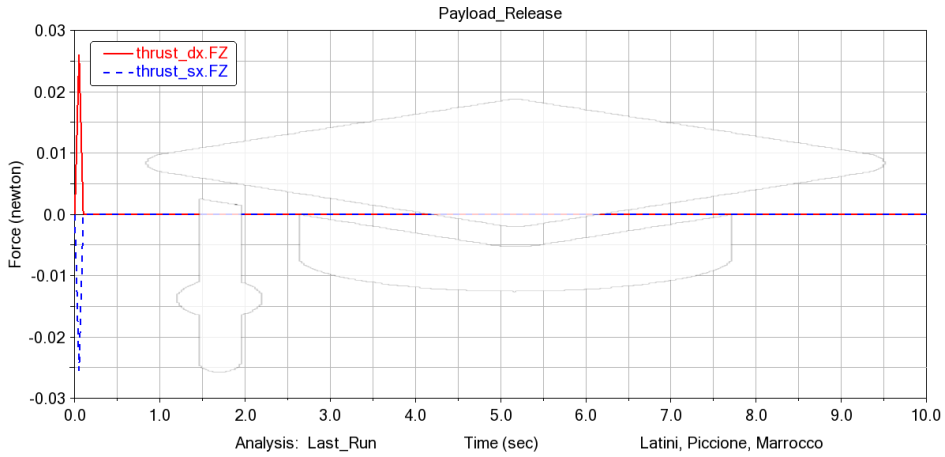

Figure 18: Thrusts components along the z-axis

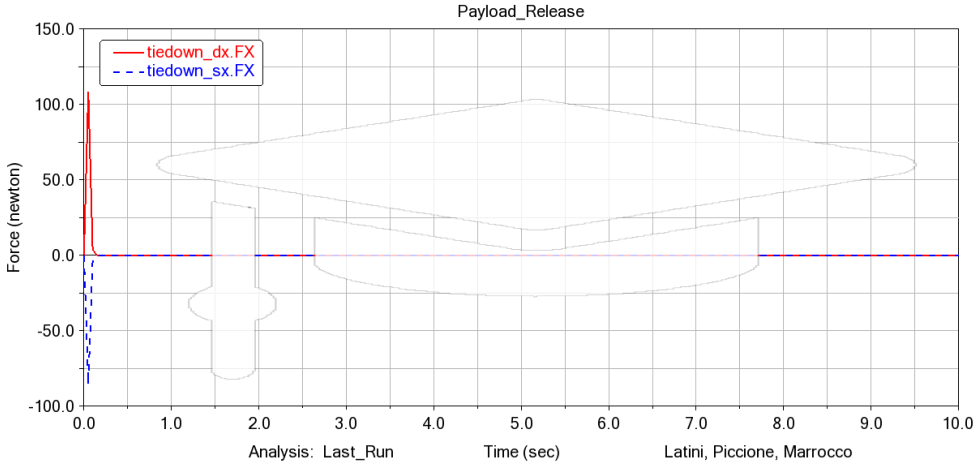

Figure 19: Tiedown forces components along the x-axis

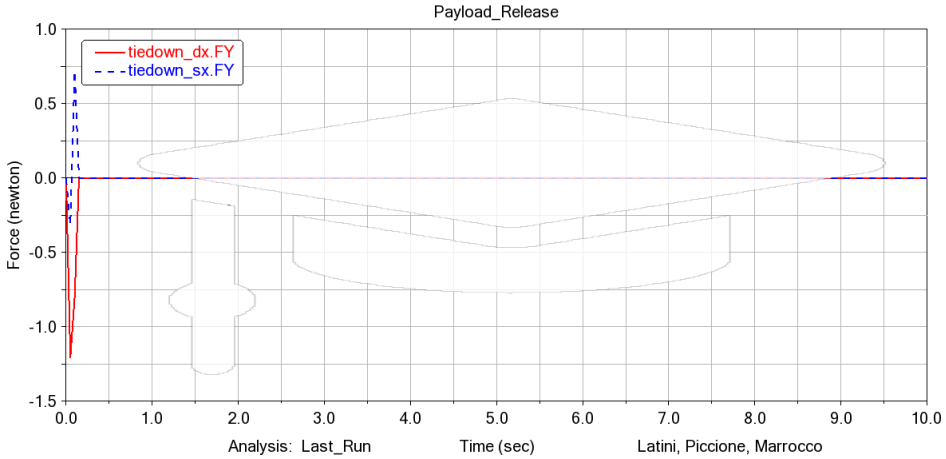

Figure 20: Tiedown forces components along the y-axis

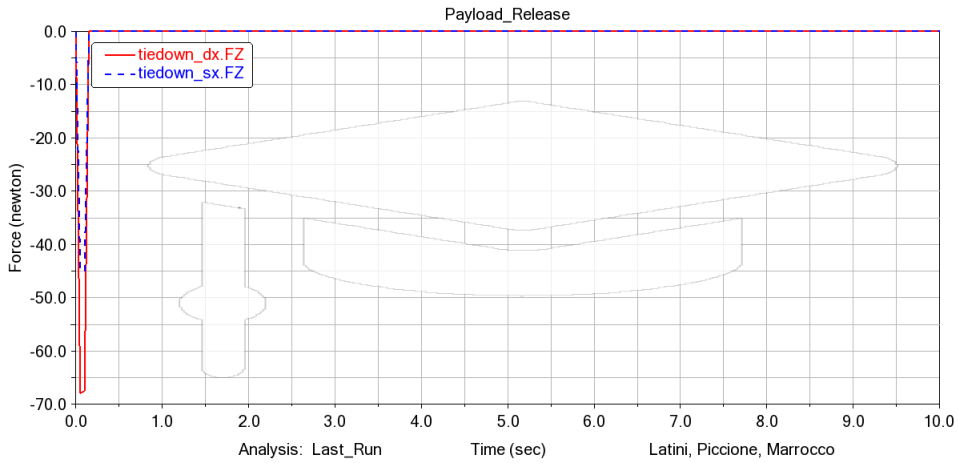

Figure 21: Tiedown forces components along the z-axis

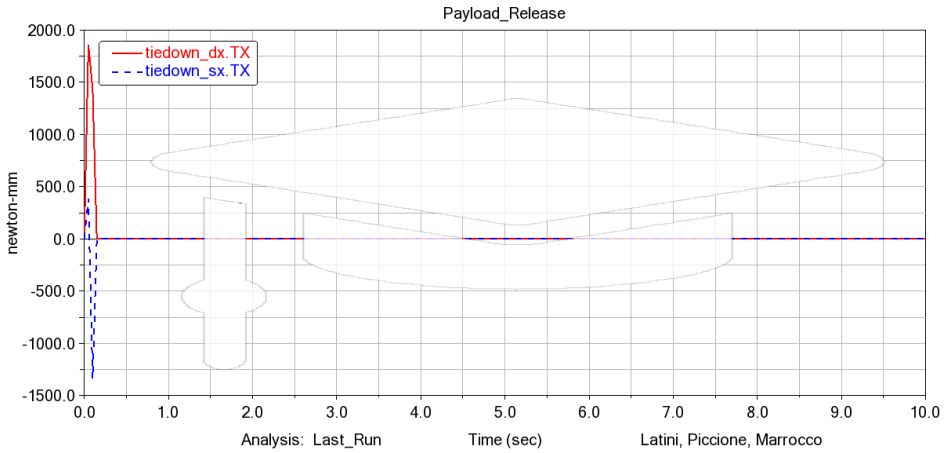

Figure 22: Tiedown torque components along the x-axis

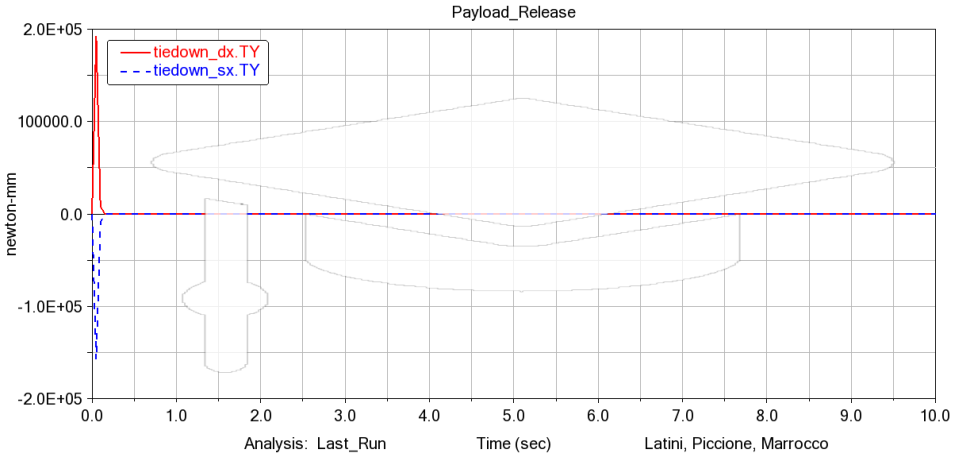

Figure 23: Tiedown torque components along the y-axis

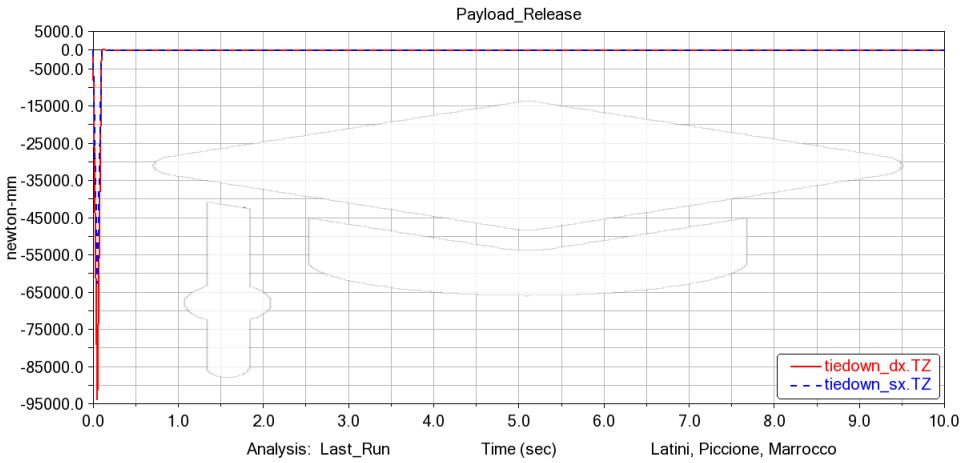

Figure 24: Tiedown torque components along the z-axis

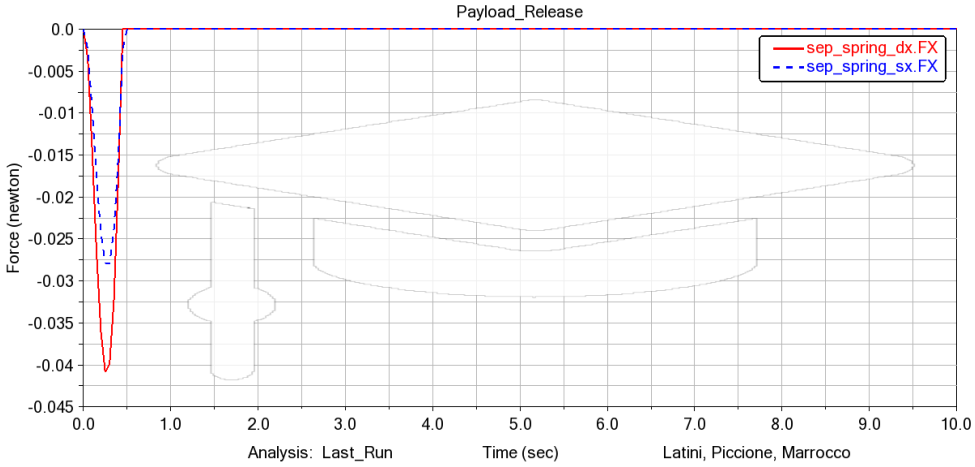

Figure 25: Push-off spring forces components along the x-axis

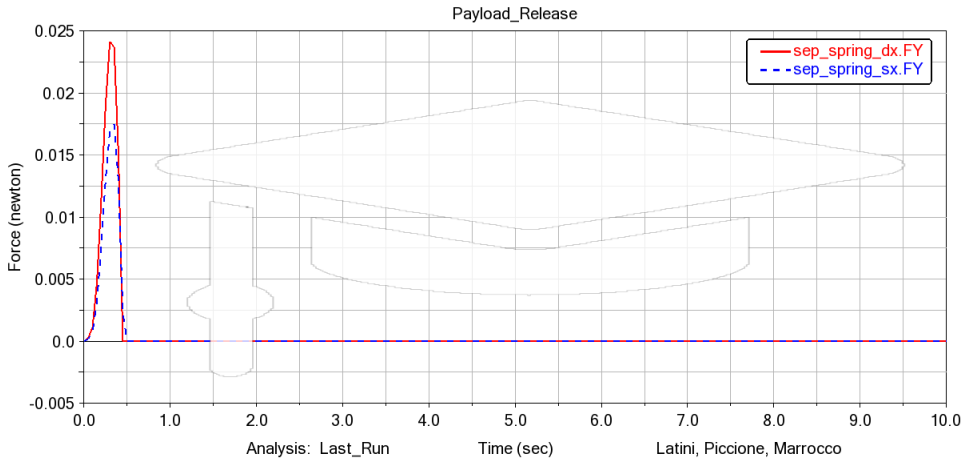

Figure 26: Push-off spring forces components along the y-axis

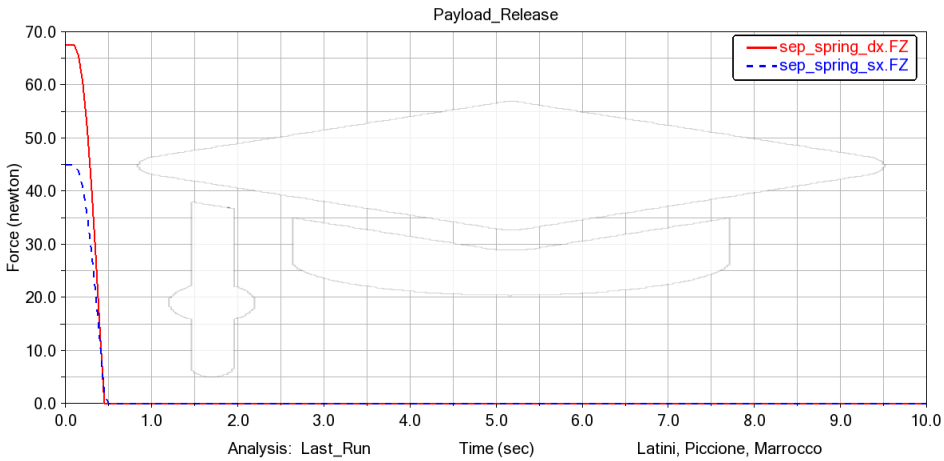

Figure 27: Push-off spring forces components along the z-axis